

Received 13 February 2025, accepted 27 February 2025, date of publication 5 March 2025, date of current version 13 March 2025.

Digital Object Identifier 10.1109/ACCESS.2025.3548424

RESEARCH ARTICLE

Auxiliary Particle Filtering With Multitudinous Lookahead Sampling for Accurate Target Tracking

**PRAVEEN B. CHOPPALA^{ID1}, (Senior Member, IEEE),
AND RAMONI ADEOGUN^{ID2}, (Senior Member, IEEE)**

¹Department of Electronics and Communication Engineering, Andhra University, Visakhapatnam 530003, India

²Department of Electronic Systems, Aalborg University, 9220 Aalborg, Denmark

Corresponding author: Praveen B. Choppala (praveenchoppala@andhrauniversity.edu.in)

This work was supported in part by the HORIZON JU-SNS-2022-STREAM-B-01-02 CENTRIC Project under Grant 101096379.

ABSTRACT The auxiliary particle filter, which is the popular extension of the standard bootstrap particle filter, is known to assist in drawing particles from regions of high probability mass of the posterior density by leveraging the incoming measurement information in the sampling process. The filter accomplishes this by looking ahead in time to determine those particles that become important when propagated forward, retract, and then propagate those particles forward in time. The key problem with this approach is that a particle determined to be important may not fall in regions of importance when actually propagated forward, either because of a large diffusion of the state transition kernel and/or a highly informative measurement, thus defeating the entire purpose of the filter. This problem leads to degeneracy. This paper proposes a method of sampling a multitude of particles for each particle to make such a decision. The key idea here is to use multiple disturbances, instead of one as does the auxiliary particle filter, as lookahead means to guide particles to regions of high probability in the posterior probability density. Through evaluation, we show that the proposed idea overcomes the said problem and exhibits less degeneracy and high tracking accuracy.

INDEX TERMS Auxiliary particle filter, lookahead particles, multitudinous sampling, resampling, target tracking.

I. INTRODUCTION

Target tracking involves the online estimation of the state $\mathbf{x}_{t=1,\dots,T}, t \in \mathbb{N}$ of a hidden moving target observed from noisy measurements $\mathbf{y}_{t=1,\dots,T}$, where t is the discrete time index. The target tracking problem can be formulated as a Bayesian filtering solution that estimates the posterior probability density function (PDF) of the target state $p(\mathbf{x}_t | \mathbf{y}_{1:t})$ by recursively using the previous state information and the current incoming measurement in estimating the current state of the target. The popularly known Bayesian filter is the particle filter (PF) that represents the posterior PDF using a set of N particles and their corresponding weights as $\{\mathbf{x}_t^i, w_t^i\}_{i=1}^N$ [1]. The PF operates by propagating a new set of

The associate editor coordinating the review of this manuscript and approving it for publication was Jolanta Mizera-Pietraszko .

particles using the Markov state transition density $p(\mathbf{x}_t | \mathbf{x}_{t-1})$ and weighing them using the measurement density $p(\mathbf{y}_t | \mathbf{x}_t)$. The use of the Markov state transition density as a proposal distribution does not include information from the incoming measurement in the sample generation process. This causes several particles to be generated from regions having low probability mass (or low weights) thus causing the filter to quickly degenerate [2], [3]. This is generally overcome by using a large number of particles and then resampling [4], [5] them so that those with low weights are stochastically replaced by those with large weights.

The auxiliary particle filter (APF) was introduced to overcome the aforementioned problem [6]. The filter uses an intelligent mechanism to include the information from the incoming measurement in the sampling process. This is done by introducing an auxiliary variable that generates,

what is called, a lookahead state for each previous particle. These lookahead states are generated from the Markov state transition density. They are then weighted using the measurement density and resampling determines which lookahead states are worthy to be retained. The filter then propagates only those previous particles determined to be important by the resampling step. This process allows the generated particles to be conditioned on both the previous particles and the incoming measurement, and hence the particle cloud will assumingly lie in regions of high probability mass. This reduces the effect of degeneracy and hence allows the use of fewer particles. Convergence results for the APF can be found in [7], [8]. The APF has found tremendous use in target tracking [9], econometrics [10] and other applications [11]. Despite minor improvements, e.g., the lookahead strategy in [12] and [13], the re-weighting in [14], equivalent weights in [15], distinct sampling in [16], optimal weighting in [17] and its convex optimisation derivation in [18], sorting methods in [20], propagation control in [19], and the nudging mechanism in [21], the methodology still remains unaltered.

A key problem, however, with the APF, is that the filter still suffers from degeneracy when particles determined to be important in the lookahead step, do not really gain importance (weight) when actually propagated forward in time. This can happen because the filter uses only one lookahead state to determine the importance of a particle drawn from the Markov state transition density. If the state transition density has a large support, then a single lookahead state is insufficient to determine a particle's importance [2]. Consequently, the propagation of the particle that was deemed important will result in it being located in a region that does not contribute probability mass to the posterior. This debilitates the purpose of the APF.

While the APF literature pertaining to its improvements and applications is rich, as aforementioned, there is limited work on explicitly overcoming the said problem. In general, [17], [18], [21] focuses on optimising the APF operation and [16] proposes to guide samples using a mixture proposal density using posterior and measurement functions. A recent work [22] addressed the said problem by correcting the lookahead sample using a regulated function of the incoming measurement and the model uncertainties. However, the accuracy of the method is highly dependent on the regulation constant, which, as a function of the measurement error, requires a large sample size for precise estimation.

In this paper, we overcome the said problem by generating a multitude of lookahead states that explore a considerable region of the state space spanned by the Markov state transition kernel. The motivating rationale for this is to leverage the transition kernel of each particle fully in determining its representativeness of exploring high probability regions when propagated forward. While the state-of-the-art APF methods use a single point mass to lookahead in time, the straightforward approach to take full advantage of the transition kernel is to sample a multitude (or read, multiple)

lookahead samples instead on one. This allows the lookahead states to be representative of a wide spectrum of state space and any decision of importance of a particle is arrived at by the multitude. This guides the propagated particles into regions that have the same support as that of the posterior PDF and hence the filter does not suffer from degeneracy as much as the APF does.

The rest of the paper is organised as follows. Section II formulates the state space model and the PF and APF filters. Then we present the proposed multitudinous APF in section III with a numerical example, followed by simulation study in section IV and concluding remarks in section V.

II. BAYESIAN PARTICLE FILTERING

The target tracking problem is generally encapsulated in the form of two mathematical equations, together called the state space model, and is described as

$$\mathbf{x}_t = f_{\Theta}(\mathbf{x}_{t-1}, \mathbf{a}_t) \quad (1)$$

$$\mathbf{y}_t = h_{\Theta}(\mathbf{x}_t, \mathbf{e}_t) \quad (2)$$

where $f(\cdot)$ and $g(\cdot)$ are the (possibly nonlinear) state transition and measurement functions, \mathbf{a}_t is the target heading disturbance (also called state transition noise) and \mathbf{e}_t is the measurement noise. The noise variables are independent and identically distributed (i.i.d.) and the parameters that govern them are included in Θ . The state transition in (1) is characterised by the Markov state transition density $p(\mathbf{x}_t | \mathbf{x}_{t-1}, \Theta)$ and the measurement equation in (2) by the measurement density $p(\mathbf{y}_t | \mathbf{x}_t, \Theta)$. We assume Θ to be known and hence discard it subsequently.

In the Bayesian context, if the posterior PDF $p(\mathbf{x}_{t-1} | \mathbf{y}_{1:t-1})$ at time $t - 1$ is available, then the posterior PDF at time t is obtained by the recursion

$$p(\mathbf{x}_t | \mathbf{y}_{1:t}) \propto \int p(\mathbf{y}_t | \mathbf{x}_t) p(\mathbf{x}_t | \mathbf{x}_{t-1}) p(\mathbf{x}_{t-1} | \mathbf{y}_{1:t-1}) d\mathbf{x}_{t-1} \quad (3)$$

which implies that the target state is propagated forward using the Markov state transition density $p(\mathbf{x}_t | \mathbf{x}_{t-1})$ embedded in the state transition function (1) and its probability is computed using the measurement density $p(\mathbf{y}_t | \mathbf{x}_t)$ embedded in the measurement function (2).

A. PARTICLE FILTERING

In situations where an analytic solution to the posterior PDF of (3) is not available, the PF is used to approximate it by casting a set of weighted particles as mixture of weighted Dirac delta functions as

$$p(\mathbf{x}_t | \mathbf{y}_{1:t}) \approx \sum_{i=1}^N w_t^i \delta(\mathbf{x}_t - \mathbf{x}_t^i) \quad (4)$$

It is desirable to draw (or generate) samples from the target density $p(\mathbf{x}_t | \mathbf{y}_{1:t})$, but since it is not possible, we draw from a proposal density which has nearly the same support as that of the target density. This is formally called importance

sampling. The target density can be described as

$$\begin{aligned} p(\mathbf{x}_t | \mathbf{y}_{1:t}) &\stackrel{(a)}{\propto} p(\mathbf{y}_t | \mathbf{x}_t, \mathbf{y}_{1:t-1}) p(\mathbf{x}_t | \mathbf{y}_{1:t-1}) \\ &\propto p(\mathbf{y}_t | \mathbf{x}_t) p(\mathbf{x}_t | \mathbf{y}_{1:t-1}) \\ &\propto \int p(\mathbf{y}_t | \mathbf{x}_t) p(\mathbf{x}_t, \mathbf{x}_{t-1} | \mathbf{y}_{1:t-1}) d\mathbf{x}_{t-1} \\ &\propto \int p(\mathbf{y}_t | \mathbf{x}_t) p(\mathbf{x}_t | \mathbf{x}_{t-1}) p(\mathbf{x}_{t-1} | \mathbf{y}_{1:t-1}) d\mathbf{x}_{t-1} \quad (5) \end{aligned}$$

where $\stackrel{(a)}{\propto}$ follows by applying Bayes' rule and (5) follows because $\mathbf{x}_t \perp\!\!\!\perp \mathbf{y}_{1:t-1} | \mathbf{x}_{t-1}$, where $\perp\!\!\!\perp$ denotes variable independence. The proposal distribution should have a support that is similar or bigger than that of the target and is chosen to factorise as

$$q(\mathbf{x}_t | \mathbf{y}_{1:t}) = q(\mathbf{x}_t | \mathbf{x}_{t-1}, \mathbf{y}_t) q(\mathbf{x}_{t-1} | \mathbf{y}_{1:t-1}) \quad (6)$$

For the given target and proposal distributions, the importance sampling process is as described in Algorithm 1.

Algorithm 1 Importance Sampling of the PF

for $i = 1$ to N **do**

 Sample lookahead particles $\bar{\mathbf{x}}_t^i \sim q(\mathbf{x}_t | \mathbf{x}_{t-1}^i, \mathbf{y}_t)$.
 Compute weights

$$\begin{aligned} \bar{w}_t^i &= \frac{p(\mathbf{x}_t | \mathbf{y}_{1:t})}{q(\mathbf{x}_t | \mathbf{y}_{1:t})} \\ &\propto \frac{p(\mathbf{y}_t | \bar{\mathbf{x}}_t^i) p(\bar{\mathbf{x}}_t^i | \mathbf{x}_{t-1}^i) p(\mathbf{x}_{t-1}^i | \mathbf{y}_{1:t-1})}{q(\bar{\mathbf{x}}_t^i | \mathbf{x}_{t-1}^i, \mathbf{y}_t) q(\mathbf{x}_{t-1}^i | \mathbf{y}_{1:t-1})} \\ &\propto w_{t-1}^i \frac{p(\mathbf{y}_t | \bar{\mathbf{x}}_t^i) p(\bar{\mathbf{x}}_t^i | \mathbf{x}_{t-1}^i)}{q(\mathbf{x}_t^i | \mathbf{x}_{t-1}^i, \mathbf{y}_t)} \quad (7) \end{aligned}$$

end for

That being said, the implementation of the proposal $q(\cdot | \cdot)$ is not straightforward as there is no convenient scheme to include the incoming measurement \mathbf{y}_t in the sampling process and hence we use the Markov state transition density as a relaxation, i.e., $q(\mathbf{x}_t | \mathbf{x}_{t-1}^i, \mathbf{y}_t) = p(\mathbf{x}_t | \mathbf{x}_{t-1})$. Then the weights in (7) become

$$\bar{w}_t^i = w_{t-1}^i p(\mathbf{y}_t | \bar{\mathbf{x}}_t^i) \quad (8)$$

The weights are then normalised. The use of the Markov state transition density does not allow the particles to be propagated to states that contribute mass to the posterior PDF, especially when the state heading disturbance is large and the incoming measurement is very informed. As a consequence, a large number of particles should be used. This again leads to a situation where most particles have small weights and very few obtain large weights. This behaviour is called *degeneracy*. We overcome this using the resampling step where we sample the indices

$$j(i) \sim \sum_{i=1}^N \bar{w}_t^i \delta(\mathbf{x}_t - \bar{\mathbf{x}}_t^i), \quad i = 1, \dots, N \quad (9)$$

That is, we chose the index $j(i)$ such that

$$P(j(i) = i) = \bar{w}_t^i \quad (10)$$

and generate a new set of weighted particles as $\mathbf{x}_t^i \leftarrow \bar{\mathbf{x}}_t^{j(i)}$ and $w_t^i = 1/N$ for $i = 1, \dots, N$. These then become the unbiased approximation of the posterior PDF as shown in (4).

B. THE AUXILIARY PARTICLE FILTER

The APF, an alternative to the PF, was proposed to enable sampling from regions of importance, or at least mimic such a process. This is achieved by first generating lookahead particles which determine those particles, when propagated, become statistically important in describing the posterior PDF, and then propagating only those to the next time step.

The posterior PDF that we aim to approximate is that of the target's at time t conditioned on all measurements received until that time step, $p(\mathbf{x}_t | \mathbf{y}_{1:t})$. The APF introduces an auxiliary variable k that guides samples into regions of importance using a lookahead step. The posterior PDF can then be written as a the marginal of the joint according to

$$p(\mathbf{x}_t | \mathbf{y}_{1:t}) = \int p(\mathbf{x}_t, k | \mathbf{y}_{1:t}) dk \quad (11)$$

The proposal distribution is factorised as

$$q(\mathbf{x}_t, k | \mathbf{y}_{1:t}) = \underbrace{q(\mathbf{x}_t | k, \mathbf{y}_t)}_{\text{Stage 2}} \underbrace{q(k | \mathbf{y}_{1:t})}_{\text{Stage 1}} \quad (12)$$

which decomposes the filtering process into two steps, (a) the lookahead step, and (b) the sampling step. In the first step, the target is defined by the marginal density

$$p(k | \mathbf{y}_{1:t}) = \int p(k, \mathbf{x}_{t-1} | \mathbf{y}_{1:t}) d\mathbf{x}_{t-1} \quad (13)$$

$$= \int p(k | \mathbf{x}_{t-1}, \mathbf{y}_{1:t}) p(\mathbf{x}_{t-1} | \mathbf{y}_{1:t}) d\mathbf{x}_{t-1}$$

$$\propto \int p(\mathbf{y}_t | k) p(k | \mathbf{x}_{t-1}) p(\mathbf{x}_{t-1} | \mathbf{y}_{1:t-1}) d\mathbf{x}_{t-1} \quad (14)$$

where (14) follows by applying Bayes' rule and because $\mathbf{y}_t \perp\!\!\!\perp \{\mathbf{y}_{1:t-1}, \mathbf{x}_{t-1}\} | \mathbf{x}_t$ and $\mathbf{x}_{t-1} \perp\!\!\!\perp \mathbf{y}_t | \mathbf{y}_{1:t-1}$.

If the proposal distribution is chosen to factorise such that

$$q(k | \mathbf{y}_{1:t}) = q(k | \mathbf{x}_{t-1}, \mathbf{y}_t) q(\mathbf{x}_{t-1} | \mathbf{y}_{1:t-1}) \quad (15)$$

with the importance distribution being chosen to be the Markov state transition prior as $q(k | \mathbf{x}_{t-1}, \mathbf{y}_t) = p(\mathbf{x}_t | \mathbf{x}_{t-1})$, then the first sampling process is defined by the two steps of Algorithm 2.

Algorithm 2 Stage 1 Importance Sampling of the APF

for $i = 1$ to N **do**

Sample lookahead particles

$$\bar{\mathbf{x}}_t^i \sim p(\mathbf{x}_t | \mathbf{x}_{t-1}^i) \quad (16)$$

Compute weights

$$\begin{aligned} \bar{w}_t^i &= \frac{p(k | \mathbf{y}_{1:t})}{q(k | \mathbf{y}_{1:t})} \\ &= \frac{p(\mathbf{y}_t | \bar{\mathbf{x}}_t^i) p(\bar{\mathbf{x}}_t^i | \mathbf{x}_{t-1}^i) p(\mathbf{x}_{t-1}^i | \mathbf{y}_{1:t-1})}{q(\bar{\mathbf{x}}_t^i | \mathbf{x}_{t-1}^i, \mathbf{y}_t) q(\mathbf{x}_{t-1}^i | \mathbf{y}_{1:t-1})} \\ &= \frac{p(\mathbf{y}_t | \bar{\mathbf{x}}_t^i) p(\bar{\mathbf{x}}_t^i | \mathbf{x}_{t-1}^i) p(\mathbf{x}_{t-1}^i | \mathbf{y}_{1:t-1})}{p(\bar{\mathbf{x}}_t^i | \mathbf{x}_{t-1}^i) q(\mathbf{x}_{t-1}^i | \mathbf{y}_{1:t-1})} \\ &\propto w_{t-1}^i p(\mathbf{y}_t | \bar{\mathbf{x}}_t^i) \end{aligned} \quad (17)$$

end for

The weights obtained from (17) are then normalised. The index $k(i)$ is then a sample from the stage 1 target density $p(k | \mathbf{y}_{1:t})$ which is expressed as a mixture density according to

$$k(i) \sim p(k | \mathbf{y}_{1:t}) \approx \sum_{i=1}^N \bar{w}_t^i \delta(\mathbf{x}_t - \bar{\mathbf{x}}_t^i), \text{ for } i = 1, \dots, N \quad (18)$$

This step gives the particle indices corresponding to time $t - 1$, which when propagated, will be guided into regions of importance. In the second stage, we leverage the particle indices obtained from the lookahead stage to generate a new set of particles and weight them according to

$$\mathbf{x}_t^i \sim p(\mathbf{x}_t^i | \mathbf{x}_{t-1}^{k(i)}) \quad (19)$$

$$w_t^i = \frac{p(\mathbf{y}_t | \mathbf{x}_t^i)}{p(\mathbf{y}_t | \bar{\mathbf{x}}_t^{k(i)})} \quad (20)$$

The weights are finally normalised.

III. PROPOSED APF WITH MULTITUDINOUS SAMPLING

In this section, we propose to generate a multitude of lookahead states per particle at time $t - 1$ and use them collectively to determine the importance of propagation of a particle. The target and proposal distributions are as shown in (11) and (12). This again decomposes the filtering problem into two stages, (a) the lookahead stage, and (b) the sampling stage. In the first stage, the target distribution can be described as

$$p(k | \mathbf{y}_{1:t}) = \prod_{i=1}^N \int p(k, \mathbf{x}_{t-1}^i | \mathbf{y}_{1:t}) d\mathbf{x}_{t-1}^i \quad (21)$$

While (13) in the APF correspond to a one-one mapping $i(t - 1) \rightarrow i(\hat{t})$ with \hat{t} denoting the lookahead stage for the t th time step, it can be observed that (21) correspond to a

one-many mapping $i(t - 1) \rightarrow j(\hat{t})$, $j = 1, \dots, M$ where $M \in \mathbb{Z}$. This implies that each i th particle corresponding to time $t - 1$ leverages on M multitudinous local samples to lookahead to time t . Then the sampling process for the i th particle, with the target density expressed as

$$\begin{aligned} &\int p(k, \mathbf{x}_{t-1}^i | \mathbf{y}_{1:t}) d\mathbf{x}_{t-1}^i \\ &\propto \int p(\mathbf{y}_t | k) p(k | \mathbf{x}_{t-1}^i) p(\mathbf{x}_{t-1}^i | \mathbf{y}_{1:t-1}) d\mathbf{x}_{t-1}^i \end{aligned} \quad (22)$$

and its proposal expressed as

$$q(k, \mathbf{x}_{t-1}^i | \mathbf{y}_{1:t}) = q(k | \mathbf{x}_{t-1}^i, \mathbf{y}_t) q(\mathbf{x}_{t-1}^i | \mathbf{y}_{1:t-1}) \quad (23)$$

results in the local importance sampling scheme derived in Algorithm 3, where the superscript i, j in $\mathbf{x}_t^{i,j}$ refers a continuum of indices $\underbrace{1, \dots, M}_{i=1}, \underbrace{1, \dots, M}_{i=2}, \dots, \underbrace{1, \dots, M}_{i=N}$.

Algorithm 3 Importance Sampling of the Proposed APF

for $i = 1$ to N **do**
for $j = 1$ to M **do**

 Sample lookahead particles $\bar{\mathbf{x}}_t^{i,j} \sim p(\mathbf{x}_t | \mathbf{x}_{t-1}^i)$.

Compute unnormalised weights

$$\begin{aligned} \bar{w}_t^{i,j} &= \frac{p(k | \mathbf{y}_{1:t})}{q(k | \mathbf{y}_{1:t})} \\ &= \frac{p(\mathbf{y}_t | \bar{\mathbf{x}}_t^{i,j}) p(\bar{\mathbf{x}}_t^{i,j} | \mathbf{x}_{t-1}^i) p(\mathbf{x}_{t-1}^i | \mathbf{y}_{1:t-1})}{q(\bar{\mathbf{x}}_t^{i,j} | \mathbf{x}_{t-1}^i, \mathbf{y}_t) q(\mathbf{x}_{t-1}^i | \mathbf{y}_{1:t-1})} \\ &= \frac{p(\mathbf{y}_t | \bar{\mathbf{x}}_t^{i,j}) p(\bar{\mathbf{x}}_t^{i,j} | \mathbf{x}_{t-1}^i) p(\mathbf{x}_{t-1}^i | \mathbf{y}_{1:t-1})}{p(\bar{\mathbf{x}}_t^{i,j} | \mathbf{x}_{t-1}^i) q(\mathbf{x}_{t-1}^i | \mathbf{y}_{1:t-1})} \\ &\propto w_{t-1}^i p(\mathbf{y}_t | \bar{\mathbf{x}}_t^{i,j}) \end{aligned} \quad (24)$$

end for
end for

This shows that the i th ancestor (particle corresponding to time $t - 1$) samples M children (lookahead particles corresponding to time t). When sampled across all $i = 1, \dots, N$ ancestor particles, the target density in (21) is collapses to a weighted approximation over MN children particles as

$$p(k | \mathbf{y}_{1:t}) \approx \sum_{i=1}^N \sum_{j=1}^M \bar{w}_t^{i,j} \delta(\mathbf{x}_t - \bar{\mathbf{x}}_t^{i,j}) \quad (25)$$

The weights in (24) are then globally normalised to sum to one. The index $j(i)$ is then a sample from the stage one target density $p(k | \mathbf{y}_{1:t})$ which is expressed as a mixture density according to

$$j(i) \sim p(k | \mathbf{y}_{1:t})$$

$$\approx \sum_{i=1}^N \sum_{j=1}^M \bar{w}_t^{i,j} \delta(\mathbf{x}_t - \bar{\mathbf{x}}_t^{i,j}), \text{ for } i = 1, \dots, N \quad (26)$$

The set of indices $\{j(i), i = 1, \dots, N\}$ are those of the lookahead children particles. The ancestors of these can be traced back by

$$k(i) = \lceil j(i)/M \rceil \quad (27)$$

This step gives the particle indices corresponding to time $t - 1$, which when propagated, will be guided into regions of importance. In the second stage, we leverage the particle indices obtained from the lookahead stage to generate a new set of particles and weight them according to

$$\mathbf{x}_t^i \sim p(\mathbf{x}_t^i | \mathbf{x}_{t-1}^{k(i)}) \quad (28)$$

$$w_t^i = \frac{p(\mathbf{y}_t | \mathbf{x}_t^i)}{p(\mathbf{y}_t | \bar{\mathbf{x}}_t^{k(i)}, \lfloor j(i)/k(i) \rfloor)} \quad (29)$$

The weights are finally normalised.

The filtering process can be summarised as follows: We generate M disturbances for each ancestor particle as $\mathbf{a}_t^{i,j} \sim p(\mathbf{a}_t)$ and obtain the M lookahead children states per ancestor particle according to

$$\bar{\mathbf{x}}_t^{i,j} = f(\mathbf{x}_{t-1}^i, \mathbf{a}_t^{i,j}) \quad (30)$$

for $j = 1, \dots, M$ and $i, 1, \dots, N$. We then compute the weights of the MN lookahead states as

$$\bar{w}_t^{i,j} = w_{t-1}^i p(\mathbf{y}_t | \bar{\mathbf{x}}_t^{i,j}) \quad (31)$$

and normalise all the weights such that all the MN weights sum to one. These lookahead states and their weights when organised as $\{\{\bar{\mathbf{x}}_t^{i,1}, \bar{w}_t^{i,1}\}, \{\bar{\mathbf{x}}_t^{i,2}, \bar{w}_t^{i,2}\}, \dots, \{\bar{\mathbf{x}}_t^{i,M}, \bar{w}_t^{i,M}\}, i = 1, \dots, N\}$ are now representative of the stage one target density of the APF, with the summation going to MN . We then resample with replacement N indices such that $P(j(i) = m) = \bar{w}_t^m, m = 1, \dots, MN$ for $i = 1, \dots, N$, after which, we sample new particles using (28) and set their weights using (29) and normalise. The proposed method is outlined in Algorithm 4.

A. NUMERICAL EXAMPLE

Here, we demonstrate the efficacy of the proposed method using a simple numerical example from $t - 1$ to t . Consider $N = 4$ univariate particles with state values $\mathbf{x}_{t-1}^{i=1, \dots, N} = \{1, 2, 3, 4\}$. Let the state transition follow a random walk model $p(\mathbf{x}_t | \mathbf{x}_{t-1}) = \mathcal{N}(\mathbf{x}_{t-1}, \tau^2 = 1)$. Assume a position observing sensor with measurement density $p(\mathbf{y}_t | \mathbf{x}_t) = \mathcal{N}(\mathbf{x}_t, \sigma^2 = 0.1)$ has produced a measurement $\mathbf{y}_t = 7$.

The APF: Suppose that the state transition in (16) result in a set of N lookahead particles $\bar{\mathbf{x}}_t^{i=1, \dots, N} = \{0.8759, 4.4897, 6.4090, 8.4172\}$. The corresponding weights obtained from (17), after normalisation, are $\bar{w}_t^{i=1, \dots, N} = \{0.0000, 0.0000, 0.9998, 0.0002\}$. Figure 1 shows the ancestor particles corresponding to time $t - 1$ and the lookahead children particles corresponding to time t . The Gaussian transition kernels for each of the ancestors are also shown. The first, second, third and fourth particles are shown in blue, red, black and green colors. The measurement is shown using a magenta triangle. The figure shows a

Algorithm 4 Proposed APF With Multitudinous Sampling

```

INPUT:  $\{\mathbf{x}_{t-1}^i, w_{t-1}^i\}_{i=1}^N$ 
OUTPUT:  $\{\mathbf{x}_t^i, w_t^i\}_{i=1}^N$ 
for  $i = 1$  to  $N$  do
    for  $j = 1$  to  $M$  do
        Generate disturbances  $\mathbf{a}_t^{i,j} \sim p(\mathbf{a}_t)$ .
        Obtain lookahead states  $\bar{\mathbf{x}}_t^{i,j} = f(\mathbf{x}_{t-1}^i, \mathbf{a}_t^{i,j})$ .
        Compute weights  $\bar{w}_t^{i,j} = w_{t-1}^i p(\mathbf{y}_t | \bar{\mathbf{x}}_t^{i,j})$ 
    end for
end for
Set  $W = 0$ .
for  $i = 1$  to  $N$  do
    for  $j = 1$  to  $M$  do
        Compute  $W = W + \bar{w}_t^{i,j}$ 
    end for
end for
for  $i = 1$  to  $N$  do
    for  $j = 1$  to  $M$  do
        Normalise  $\bar{w}_t^{i,j} = \frac{\bar{w}_t^{i,j}}{W}$ 
    end for
end for
Resample  $j(i) \sim \sum_{n=1}^N \sum_{m=1}^M \bar{w}_t^{n,m} \delta(\mathbf{x}_t - \bar{\mathbf{x}}_t^{n,m})$  for  $i = 1, \dots, N$ 
for  $i = 1$  to  $N$  do
    Ancestor trace  $k(i) = \lceil j(i)/M \rceil$ 
    Generate particles using (28).
    Compute weights using (29).
end for
Set  $W = 0$ .
for  $i = 1$  to  $N$  do
    Compute  $W = W + w_t^i$ .
end for
for  $i = 1$  to  $N$  do
    Normalise  $w_t^i = \frac{w_t^i}{W}$ 
end for

```

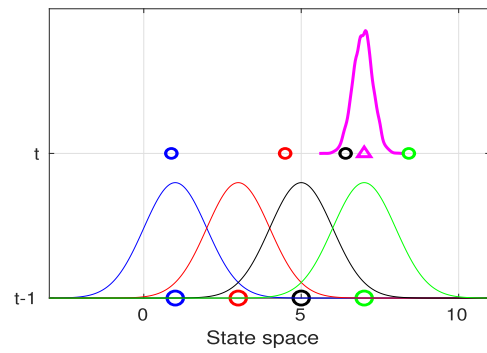


FIGURE 1. Illustration of the time transition of $N = 4$ particles for the APF. The circles are the particles. The thin solid lines are the transition kernels. The magenta triangle is the measurement. The magenta solid line is the true posterior simulated using 1000 particles.

classic case where the APF fails in using its lookahead stage to determine important particles. Since the APF draws

one lookahead for one ancestor particle, it could lead to a case where the lookahead sample could lie close to the measurement and hence obtain a large weight, but since its transition kernel does not span the true region of importance, the corresponding ancestor particle may not fall in regions of importance when actually propagated using (19). This case can be seen in the figure, where the third particle (in black) falls close to the measurement and grabs a large weight of 0.9998 but its transition kernel does not efficiently span the region of importance of the posterior PDF (shown in magenta and simulated using 1000 particles). It can be observed that the kernel density of the fourth particle (in green) spans the posterior effectively but it has obtained a very low weight as its lookahead sample was not close to the measurement. The effect of this phenomena can otherwise be studied by observing the probability of survival of the lookahead particles, defined by number of times the index $k(i)$ is resampled from the mixture density

$$\begin{aligned} k(i) \sim & 0.0000\delta(\mathbf{x}_t - 0.8759) + 0.0000\delta(\mathbf{x}_t - 4.4897) \\ & + 0.9998\delta(\mathbf{x}_t - 6.4090) + 0.0002\delta(\mathbf{x}_t - 8.4172) \end{aligned}$$

These survival probabilities, averaged over 1000 iterations, are

$$\begin{aligned} p_S(k(i=1, \dots, N)=1) &= 0 \\ p_S(k(i=1, \dots, N)=2) &= 0 \\ p_S(k(i=1, \dots, N)=3) &= 0.9995 \\ p_S(k(i=1, \dots, N)=4) &= 0.0005 \end{aligned}$$

and it can be observed that the output of the APF does not truly reflect into the regions of importance in the posterior PDF.

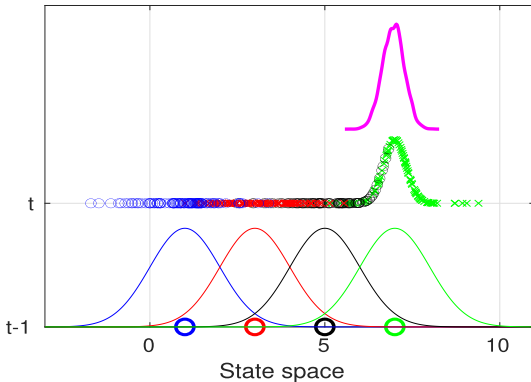


FIGURE 2. Illustration of the time transition of $N = 4$ particles for the proposed method. The specifications of Figure 1 apply to this also. The x , x , \circ at time t are the weighted lookahead multitudinous particles.

Proposed method: The proposed method is run with $M = 100$ children particles for each of the $N = 4$ ancestor particles. These children are plotted in different colors in Figure 2 at time t . It can be observed that leveraging the decision on multitudinous sampling, instead on one sample, reflects that the fourth particle (in green), when propagated,

has a higher chance of being located in regions of importance of the posterior. The survival probabilities, averaged over 1000 iterations, are

$$\begin{aligned} p_S(k(i=1, \dots, N)=1) &= 0 \\ p_S(k(i=1, \dots, N)=2) &= 0.0003 \\ p_S(k(i=1, \dots, N)=3) &= 0.1780 \\ p_S(k(i=1, \dots, N)=4) &= 0.8217 \end{aligned}$$

This gives more credence to the fourth particle which when propagated has a higher chance of being located in regions that truly contribute to the posterior. The proposed method can be straightforwardly applied to the general class of PFs that involve lookahead samples for an accurate representation of the posterior, for e.g., [12], [13], and [17], or the marginalised and regularised filters, and also for other applications including track-before-detect and joint multiple target tracking.

IV. EVALUATION STUDY

In this section we present the simulation results for the proposed method. All the results of this paper are averaged over 1000 Monte Carlo iterations.

A. NONLINEAR GROWTH MODEL

Here we use the well known nonlinear growth model to compare the proposed method with the PF [1] and the APF [6]. The nonlinear state space model is given by

$$\mathbf{x}_t = \frac{\mathbf{x}_{t-1}}{2} + \frac{25\mathbf{x}_{t-1}}{1 + \mathbf{x}_{t-1}^2} + 8\cos(1.2 t) + a_t \quad (32)$$

$$\mathbf{y}_t = \frac{\mathbf{x}_t^2}{20} + e_t \quad (33)$$

for $t = 1, \dots, T$, where the heading disturbance is $a_t \sim \mathcal{N}(0, \tau^2)$ and the observation noise is $e_t \sim \mathcal{N}(0, \sigma^2)$ and the total number of time steps is $T = 500$. The model parameters are $\Theta = (\tau^2 = 10, \sigma^2 = 1)$. The number of particles is set to $N = 20$.

Figure 3 shows the root mean square error (RMSE) versus the number of multitudinous particles M for each particle. It can be observed that when $M = 1$, the proposed filter is equivalent to the APF and hence its RMSE is close to that of the APF. As M increases, the lookahead effect of the multitudinous sampling sets in and the proposed filter tracks more effectively than the APF. However, it can be seen that performance becomes asymptotic from $M > 5$. The APF and the PF have no bearing on the value of M and hence their RMSE values remain unchanged $\forall M$. The reason for the proposed method to exhibit higher tracking accuracy is that the sampled particles are made to explore regions of high probability density within the posterior PDF by virtue of sampling multiple copies.

Secondly, we test the tracking accuracy of the proposed filter for varying noise levels. Figure 4 shows the RMSE

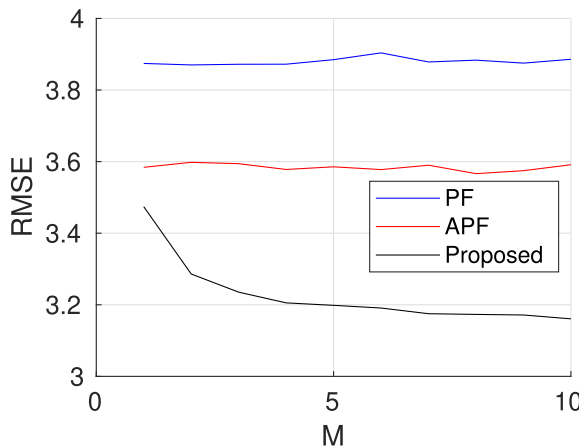


FIGURE 3. The RMSE versus the value of M .

versus the measurement noise variance σ^2 when $N = 20$ and $M = 5$. It can be observed that the proposed filter exhibits nearly 11.26% decrease in RMSE over the APF and the value is maintained for all the values of σ^2 . The key reason for this is the ability of the filter to generate particles that possess meaningful information in their weights that contributes to the filter accuracy. The PF and the APF do not perform as good as the proposed does because they fail to include the incoming measurement in propagating particles along time.

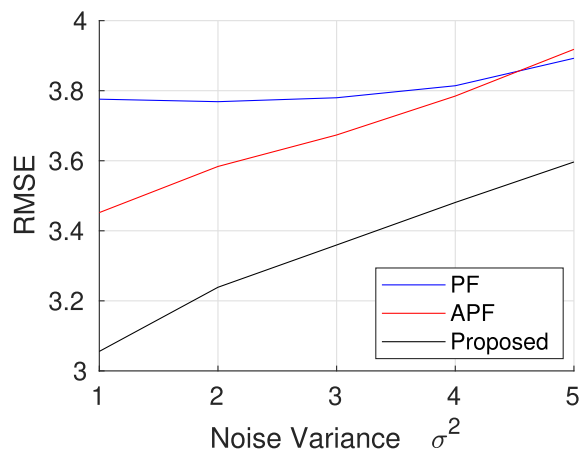


FIGURE 4. The RMSE versus the noise variance σ^2 .

The merit of using multitudinous states as opposed to one lookahead state is to guide particles into regions of high probability mass, which in turns makes every particle have a meaningful semblance of the posterior PDF. A direct result of this feature is reduced degeneracy. Degeneracy in the PFs is measured as the estimated effective sample size given by

$$\text{ESS} = 1 / \sum_{i=1}^N (\omega_t^i)^2 \quad (34)$$

Figure 5 shows the estimated ESS for all the 500 time instances for $M = 1, 10$ and it can be observed that the

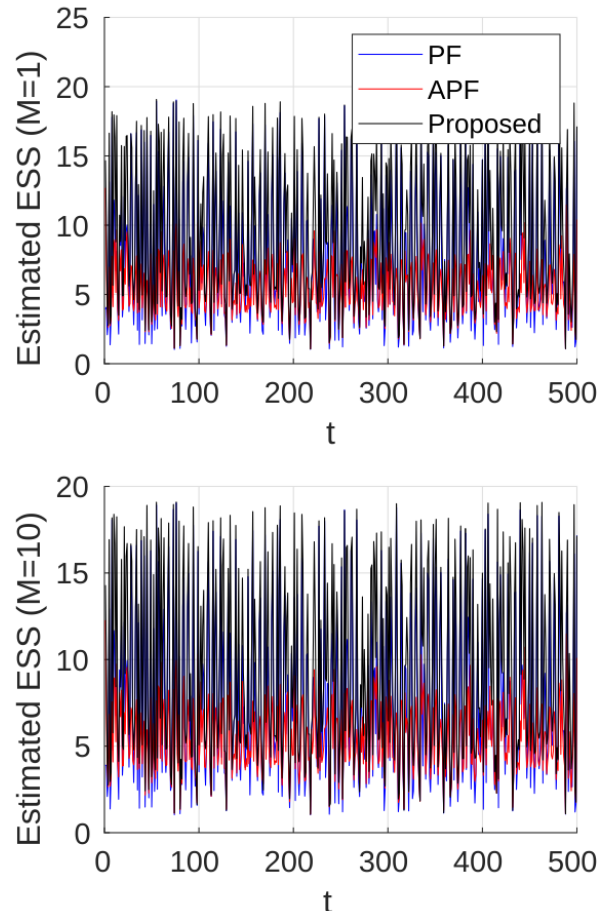


FIGURE 5. The estimated effective sample size versus the time index t . The legend of the top panel applies to the bottom also.

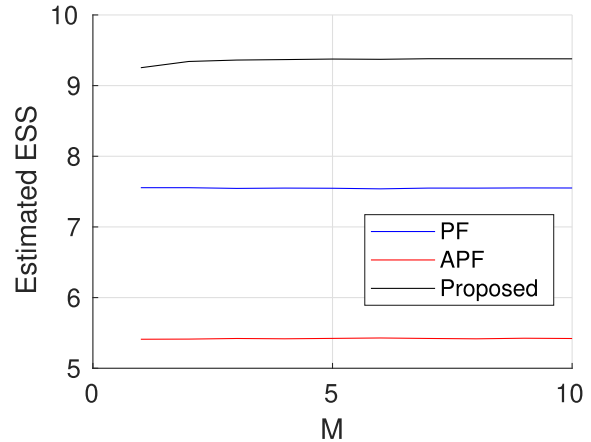


FIGURE 6. The estimated effective sample size versus the value of M .

proposed filter exhibits the highest ESS. Figure 6 shows the average estimated ESS versus the M and it can be seen that the proposed filter achieves the highest value over and beyond the APF and the PF.

In Figure 7, we show the estimated ESS versus the noise variance σ^2 . It can be observed that when $\sigma^2 = 1$, the

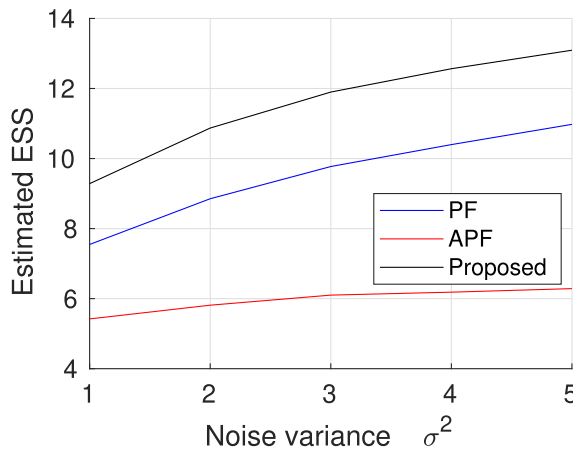


FIGURE 7. The estimated effective sample size versus the noise variance σ^2 when $N = 20$ and $M = 5$.

result is nearly close to that of the estimated ESS shown in the Figure 6 and as σ^2 increases, the estimated ESS of the proposed method also increases. It can be noted that the APF exhibits extremely high degeneracy within its particles, purportedly defeating the purpose it was proposed for, the key reason for which is that the single lookahead state has not truly contributed enough in determining the importance particles and the following retraction and propagation steps only worsens the output. The PF does not suffer as much as the APF since it does not have the retract and propagation steps, but it uses the lookahead states and the propagated particles. This outcome, by all means, results in the proposed method having higher weight aggregate value than that of the APF, which is shown in Figure 8. The figure shows the average weight of each particle over the 500 time steps and it can be observed that the proposed method, by virtue of sampling particles from regions of high importance, has higher weights. While the aggregate weight of the APF was found to be 0.000975 when averaged over all the time steps, the same of the proposed method was found to be 0.0029, indicating that the particles indeed explore regions with high weight (probability mass).

B. LIKELIHOOD ANALYSIS

Here, we verify the likelihood convergence of the proposed filter. Assume an auto regressive linear Gaussian model of order one described by

$$p(\mathbf{x}_t | \mathbf{x}_{t-1}) = \mathcal{N}(\phi \mathbf{x}_{t-1}, \tau^2) \quad (35)$$

$$p(\mathbf{y}_t | \mathbf{x}_t) = \mathcal{N}(\mathbf{x}_t, \sigma^2) \quad (36)$$

The Kalman filter provides a optimal analytic solution to the estimation of the target state from its observables by constructing a Gaussian probability density of the state with respect to the measurements. For the model specified above, the initial mean is $\mathbf{x}_{t=0} = 0$ and the initial variance is $\mathbf{s}_{t=0} = \tau^2/(1 - \phi^2)$. The posterior PDF of the target state

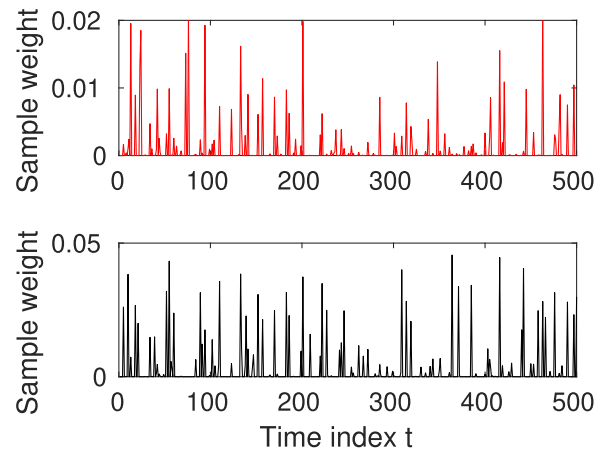


FIGURE 8. The (average value of the) normalised weights versus the time index. The top panel corresponds to the APF and the bottom to the proposed filter. We set $\sigma^2 = 1$.

at time t , obtained by integrating the previous state, is given by

$$p(\mathbf{x}_t | \mathbf{y}_{1:t}) = \frac{p(\mathbf{y}_t | \mathbf{x}_t)p(\mathbf{x}_t | \mathbf{y}_{1:t-1})}{p(\mathbf{y}_t | \mathbf{y}_{1:t-1})} \quad (37)$$

$$= \frac{\int p(\mathbf{y}_t | \mathbf{x}_t)p(\mathbf{x}_t | \mathbf{x}_{t-1})p(\mathbf{x}_{t-1} | \mathbf{y}_{1:t-1})d\mathbf{x}_{t-1}}{p(\mathbf{y}_t | \mathbf{y}_{1:t-1})} \quad (38)$$

The likelihood function (conditioned on all model parameters, which is not shown for convenience) is given by

$$p(\mathbf{y}_{1:T}) = \prod_{t=1}^T p(\mathbf{y}_t | \mathbf{y}_{1:t-1}) \quad (39)$$

where the likelihood function corresponding to time t is given by the normalisation constant (the denominator term) in the posterior PDF in (38). This can be derived as

$$\begin{aligned} p(\mathbf{y}_t | \mathbf{y}_{1:t-1}) &= \int p(\mathbf{y}_t | \mathbf{x}_t)p(\mathbf{x}_t | \mathbf{y}_{1:t-1})d\mathbf{x}_t \\ &= \int \int p(\mathbf{y}_t | \mathbf{x}_t)p(\mathbf{x}_t | \mathbf{x}_{t-1})p(\mathbf{x}_{t-1} | \mathbf{y}_{1:t-1}) \\ &\quad d\mathbf{x}_t, d\mathbf{x}_{t-1} \\ &\approx \int p(\mathbf{y}_t | \mathbf{x}_t) \left(\sum_{i=1}^N w_{t-1}^i \delta(\mathbf{x}_t - \bar{\mathbf{x}}_t^{i,j}) \right) d\mathbf{x}_t \\ &\approx \sum_{i=1}^N w_{t-1}^i p(\mathbf{y}_t | \bar{\mathbf{x}}_t^{i,j}), \text{ for any } j \in (1, M) \end{aligned} \quad (40)$$

All the probability densities in the proposed method are represented using a fixed set of N particles. The additional $NM - N$ samples, over the fixed sample size N , are supplementary and assistive in exploring the state space more effectively. Therefore it suffices to take any one value of $j \in (1, M)$ for each parent i as a candidate for the computation of the likelihood estimate.

Figure 9 shows the log likelihood estimate of the filters for varying numbers of particles (on log scale). The proposed

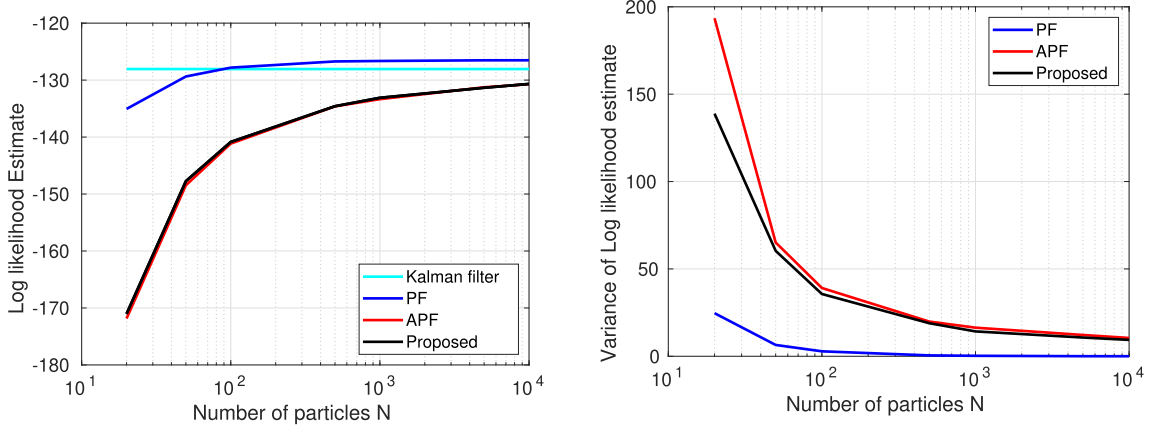


FIGURE 9. The left panel shows the log likelihood estimate versus the number of particles and the right panel shows the variance of the log likelihood estimate versus the number of particles.

method is implemented with $M = 10$. It can be observed that the particle filters' estimation approaches the true value of the likelihood (given by the optimal solution Kalman filter) for increasing numbers of particles. The figure also shows the variance of the log likelihood estimate and it can be observed that the variance in all the filters decreases asymptotically with the number of particles. It is noteworthy that the proposed solution conforms to the solution of the conventional APF in the truest sense of accurate representation of the Bayesian posterior PDF, which can be inferred by observing its conformity with the likelihood estimate and the corresponding variance estimate. It is thus fair to say the proposed method gives an unbiased estimate of the likelihood function.

C. APPLICATION TO RADAR TARGET TRACKING

In this section, we consider the example of airborne tracking using ground moving target indicator (GMTI) radar (for reference, see Ch. 10 of [3]). Let the target dynamics be encapsulated in the target state vector at time t as $\mathbf{x}_t = (x_t, x_i, y_t, y_i)^\top$ where (x_t, y_t) denote the positions and (x_i, y_i) the velocities of the target. We employ a constant velocity (CV) model to define the discrete kinematic characteristics of the target state transition as

$$\mathbf{x}_t = \mathbf{F}\mathbf{x}_{t-1} + \mathbf{G}\mathbf{a}_t \quad (41)$$

where the matrices \mathbf{F} and \mathbf{G} respectively are

$$\mathbf{F} = \begin{bmatrix} 1 & \delta t & 0 & 0 \\ 0 & 1 & 0 & 0 \\ 0 & 0 & 1 & \delta t \\ 0 & 0 & 0 & 1 \end{bmatrix}, \quad \mathbf{G} = \begin{bmatrix} \delta t & 0 & 0 & 0 \\ 0 & \delta t/2 & 0 & 0 \\ 0 & 0 & \delta t & 0 \\ 0 & 0 & 0 & \delta t/2 \end{bmatrix}$$

where $\delta t = 1$ second is the duration between two discrete measurements. The target heading disturbance variable is defined as $\mathbf{a}_t \sim \mathcal{N}(\mathbf{0}, \mathbf{Q}_t)$ with the covariance matrix being $\mathbf{Q}_t = \text{diag}(\tau_p^2, \tau_v^2, \tau_p^2, \tau_v^2)$ where (τ_p^2, τ_v^2) are the (fixed)

variances along the position and velocity axes. We set $\tau_p^2 = \tau_v^2 = 0.01^2$ m/sec.

We employ a single GMTI observer, whose initial position and velocities are $\mathbf{x}_{0t} = (0, 0, 0, 0)^\top$ and moves according to the model described in (41), and generates noisy measurements of the range ρ , the azimuth θ and the Doppler ρ according to

$$\mathbf{y}_t = \begin{bmatrix} \rho_t \\ \theta_t \\ \rho_t \end{bmatrix} = \begin{bmatrix} \sqrt{(x_t - xo_t)^2 + (y_t - yo_t)^2} \\ \tan^{-1}(x_t - xo_t)/y_t - yo_t \\ (x_t - xo_t)x_t + (y_t - yo_t)y_t \\ \sqrt{(x_t - xo_t)^2 + (y_t - yo_t)^2} \end{bmatrix} + \mathbf{e}_t \quad (42)$$

for $t = 1, \dots, T$, where (xo_t, yo_t) is the position of the observer at time t and the measurement noise is defined as $\mathbf{e}_t \sim \mathcal{N}(\mathbf{0}, \mathbf{R})$ with $\mathbf{R} = \text{diag}(\sigma_\rho^2, \sigma_\theta^2, \sigma_\rho^2)$. We set the noise variance corresponding to the range as $\sigma_\rho^2 = 5$ m/sec, the noise variance corresponding to the azimuth as $\sigma_\theta^2 = 0.01$ rad/sec, and the noise variance corresponding to the Doppler as $\sigma_\rho^2 = 1$ cycles/sec.

We use four test measures to evaluate the performance of the proposed method against the standard PF [1], the APF [6], and the recently proposed IAPF [17], SWLAPF [20], the NPF [21] and the IAPF2021 [22]. Each of the performance metrics are defined as follows. The time averaged root mean square error (RMSE) is

$$\text{RMSE} = \frac{1}{T} \sum_{t=1}^T \sqrt{(x_t - \hat{x}_t)^2 + (y_t - \hat{y}_t)^2} \quad (43)$$

A low value of RMSE is desired and indicates high tracking accuracy. The second performance metric is the estimated effective sample size (ESS), defined as

$$\hat{N}_{\text{eff}} = \frac{1}{T} \sum_{t=1}^T \sum_{i=1}^N \frac{1}{(w_t^i)^2} \quad (44)$$

TABLE 1. This table shows average values of the RMSE, the \hat{N}_{eff} , the % number of divergent tracks and the fail probability of the various filters for varying numbers of particles N for the model in (41) and (42). The proposed method is implemented with $M = 10$.

N	$N = 20$	$N = 20$	$N = 50$	$N = 50$	$N = 100$	$N = 100$
Measure	$E(\text{RMSE})$	$V(\text{RMSE})$	$E(\text{RMSE})$	$V(\text{RMSE})$	$E(\text{RMSE})$	$V(\text{RMSE})$
PF	0.8342	0.7999	0.5121	0.3543	0.3829	0.1804
APF	0.5927	0.3398	0.3732	0.1003	0.3013	0.0458
IAPF	0.6563	0.3891	0.4853	0.2082	0.4066	0.3563
SWLAPF	0.8872	1.7747	0.4780	0.4537	0.4008	0.3563
NPF	0.6158	0.3432	0.3785	0.1213	0.3115	0.0667
IAPF2021	0.6228	0.3412	0.3945	0.1200	0.3215	0.0655
Prop. ($M = 10$)	0.5522	0.2569	0.3567	0.1167	0.2697	0.0453
Measure	$E(\hat{N}_{\text{eff}})$	$V(\hat{N}_{\text{eff}})$	$E(\hat{N}_{\text{eff}})$	$V(\hat{N}_{\text{eff}})$	$E(\hat{N}_{\text{eff}})$	$V(\hat{N}_{\text{eff}})$
PF	17.8246	8.1542	43.8369	13.2278	86.2584	35.9947
APF	19.8429	3.5089	49.8575	9.1152	99.7853	18.0390
IAPF	18.5563	3.5582	45.9953	8.6286	91.5281	19.7222
SWLAPF	16.5719	1.5223	40.4178	1.9135	75.9067	5.3003
NPF	19.5220	3.5203	49.7625	9.0012	99.5521	18.1371
IAPF2021	19.5156	3.5530	49.7602	10.9734	99.7951	18.5921
Prop. ($M = 10$)	19.9044	3.8743	49.8321	9.0137	99.8204	18.6908
Measure	$E(\text{NDT})$	$E(\text{FP})$	$E(\text{NDT})$	$E(\text{FP})$	$E(\text{NDT})$	$E(\text{FP})$
PF	0.2470	0	0.1100	0	0.0550	0
APF	0.1477	0.0622	0.0494	0.0401	0.0141	0.0144
IAPF	0.1749	0.1469	0.0987	0.1018	0.0523	0.0551
SWLAPF	0.2185	0.1504	0.0666	0.0728	0.0349	0.0340
NPF	0.1800	0.0759	0.0414	0.0526	0.0176	0.0152
IAPF2021	0.1883	0.0700	0.0688	0.0755	0.0261	0.0290
Prop. ($M = 10$)	0.1304	0.0493	0.0401	0.0312	0.0106	0.0061

The value of the estimated ESS is desired to be close to N as it indicates less degeneracy within the filter estimate. The third metric is the number of divergent tracks (NDT), defined as average number of times the RMSE value is over 1m. The fourth metric is the fail probability (FP), defined as the average number of times the filter loses complete track, i.e., if its RMSE goes over 3m and stays so until the last time step or if the filter suffers from divide by zero errors; this scenario requires the radar operator to manually reset the filter. Again, all the results are an average over 1000 Monte Carlo iterations.

Table 2 shows the values of each of the four metrics for varying numbers of multitudinous samples (children) per particle, M , for the proposed method. In addition to the average mean values, the table also shows the Monte Carlo variance of the RMSE and the estimated ESS metrics. It is apparent that the $M = 1$ case is equivalent to the APF. It can be observed that as the value of $M \uparrow$ increases, the filter degeneracy reduces ($\hat{N}_{\text{eff}} \downarrow$) as a consequence of having more

particles in regions of high importance probability. The error reduces RMSE \downarrow as the quality of particles representing the posterior increases. Consequently, the number of divergent tracks decreases NDT \downarrow . The major culprit for the high fail probability of the APF (the $M = 1$ case) is the divide by zero errors caused when the state transition noise is much higher than the measurement noise and when particles fail to localise in regions of high posterior probability during the final sampling stage. This problem can only be overcome by employing a second resampling step within the APF, which is out of question for all practical purposes. Nevertheless, we observe that as M increases the proposed filter fails less often as the said problem is being incrementally overcome. We have observed that all values become asymptotic as M increases further, and hence not shown.

Table 1 shows the values of the performance metrics for varying numbers of particles. As with the APF, it is expected that the proposed methodology operate on fewer numbers of particles. Accordingly, we observe that the proposed

TABLE 2. This table shows the RMSE, the \hat{N}_{eff} , the % number of divergent tracks and the fail probability of the proposed method for varying numbers of the samples per particle M with the number of total particles fixed at $N = 20$ for the model in (41) and (42).

Measure	$M = 1$	$M = 5$	$M = 10$	$M = 20$
$E(\text{RMSE})$	0.5874	0.5600	0.5522	0.5265
$V(\text{RMSE})$	0.2972	0.2903	0.2569	0.2312
$E(\hat{N}_{\text{eff}})$	19.8477	19.8828	19.9044	19.9247
$V(\hat{N}_{\text{eff}})$	3.5966	3.6218	3.8743	3.9148
$E(\text{NDT})$	0.1436	0.1376	0.1304	0.1297
$E(\text{FP})$	0.0583	0.0502	0.0493	0.0433

method with $M = 1$ performs comparatively with the APF and the IAPF. The OAPF showed results similar to the IAPF and is hence not shown. As N increases, all the methods exhibit incrementally improved performance in all four measures. That being said, all the APFs still suffer from the problem of picking the wrong candidate for propagation based on a single lookahead sample. The IAPF-2021, although satisfactory, has been found to be highly susceptible to the choice of the constants in the regulation and resampling steps. The proposed method, on the other hand, at $M = 10$, shows improvement over the others by virtue of picking the right candidates for propagation.

Since the proposed filter uses M lookahead particles per parent particle to enhance tracking performance, it is critical to analyse the corresponding trade-off in the computational time. For the test case of Table 1 with $N = 20$, Figure 10 shows the RMSE versus the computational time for all the filters. We define it to be the run time of each of the filters at a single time instant, implemented using Matlab Online on a Apple M2 computer with 8GB RAM. The proposed filter, implemented for $M = 1, 5, 10, 20$, is shown using a solid black line, while the others are shown using colored dots (as M is irrelevant). It can be observed that as M increases, the proposed filter requires more computation than the PF, the APF and the SWLAPF, but achieves superior tracking accuracy than all filters, and the trade-off can be decided from the plot. The IAPF and the NPF, albeit being similar to the APF in RMSE, are computationally expensive due to lookahead and weight calculations, and the IAPF2021 due to additional correction steps.

Table 3 shows the tracking error for different noise variances along the range σ_{ρ}^2 , azimuth σ_{θ}^2 and Doppler $\sigma_{\dot{\rho}}^2$ for $N = 20$ and $M = 10$. The table shows the RMSE profile of the filters and it can be observed that the proposed filter at $M = 10$ outperforms the state-of-the-art with fewer particles by virtue of having samples placed in regions of the posterior that have high probability mass. It is noteworthy that the increase in the noise across the range increases the error in all the filters, as the range contributes to the position estimate of the filters. Contrarily, the noise along the bearing

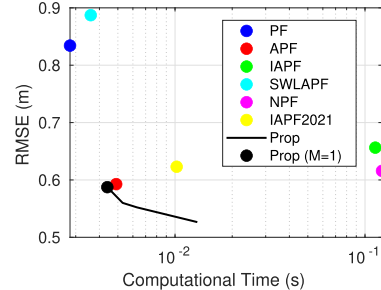


FIGURE 10. The RMSE (in meters) versus the computational time (in seconds) for the filters under test and the proposed filter at $N = 20$ particles. The proposed method is shown at $M = 1, 5, 10, 20$ and the value corresponding to $M = 1$ is shown using a black dot.

TABLE 3. This table shows the RMSE for different noise variance values of the range and doppler measurements. The azimuth error variance is fixed at $\sigma_{\theta}^2 = 0.01$. The number of particles is $N = 20$ and for the proposed filter, $M = 10$.

Measure	Case 1	Case 2	Case 3	Case 4
$(\sigma_{\rho}^2, \sigma_{\dot{\rho}}^2)$	(5,1)	(1,1)	(1,3)	(5, 3)
PF	0.8376	0.7898	0.7164	0.7908
APF	0.5771	0.5041	0.4182	0.5660
IAPF	0.6401	0.5529	0.4778	0.6616
SWLAPF	0.8992	0.9332	0.5802	1.1488
NPF	0.6201	0.5129	0.4378	0.6316
IAPF2021	0.6221	0.5287	0.4453	0.6423
Proposed	0.5575	0.4562	0.3893	0.5008

measurement will cause an error in the angle estimate of the filters.

As an illustration, Figure 11 shows the particle clouds of the filters a single simulation run for the above specifications. The number of particles is $N = 20$ and the number of multitudinous samples in the proposed method is $M = 10$. The own ship stays at the origin $(0, 0)$. The filters are implemented with the constant velocity motion model which is a practical choice for real world tracking scenarios. The ground truth target, however, starts at $(0, 0)$ and moves anti-clockwise for 100 seconds reaching where it had started. This scenario accounts for model mismatch in the state dynamics, especially during the moments immediately succeeding the firing of missile, where the weapon makes one or few manoeuvres before stabilising, and hence tests for the robustness of the filter. It can be observed that the PF and the APF diverge often whenever there is a deviation from constant velocity as there are not sufficient particles to explore the state space. This problem is overcome, in practice, by manually reinitialising the filter by a radar operator. The proposed method overcomes this problem as it leverages on multitude of samples per particle to lookahead the probable regions of high importance of the posterior PDF. Therefore, it does not suffer from track divergence and produces accurate solution.

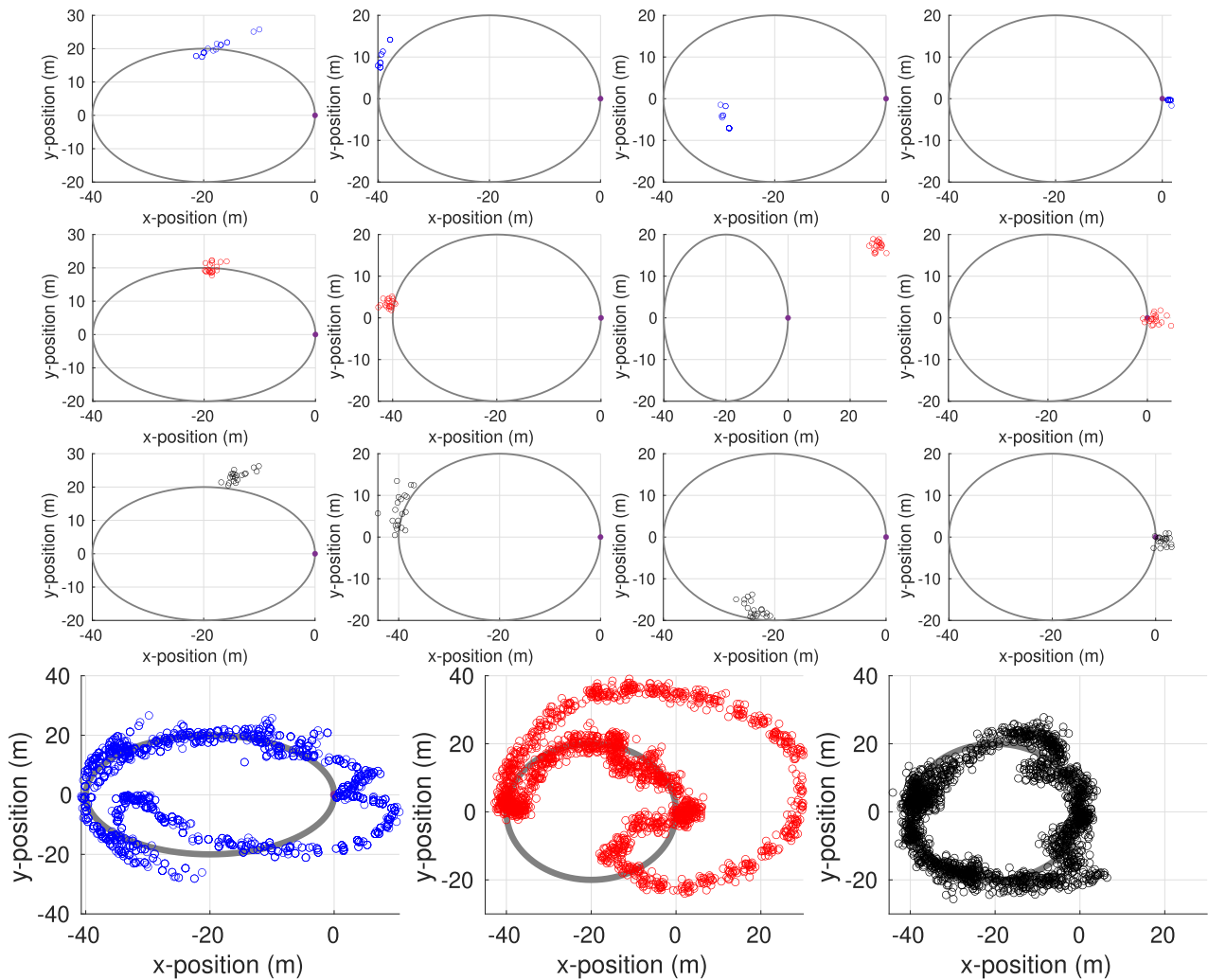


FIGURE 11. A simulation of the particle clouds of the filters. The first three rows correspond to the PF (in blue), the APF (in red) and the proposed method (in black) respectively and the four columns therein correspond to time steps $t = 25, 50, 75$ and 100 respectively. The fourth row shows the particle clouds corresponding to all the time steps with the columns therein corresponding to the PF, the APF and the proposed methods. The ground truth is shown in black solid line. The initial position of a moving observer is shown as a solid dot.

V. CONCLUSION

This paper developed a multitudinous sampling approach that overcomes the challenges in the traditional APF, that the particles once determined to be important, when propagated, do not really gain importance weight. A key fundamental cause for this problem is that relying on one lookahead sample to arrive at a decision about the importance of a particle in being propagated forward is insufficient. This paper proposed a scheme to rely on a multitude of lookahead samples, instead of one, to make a collective decision about propagating a particle to the next time step. Three state space models, including a linear Gaussian model, have been used to diversify the validation of our proposal, and it has been found that the method gives an unbiased estimate of the likelihood function and also resulted in reduced degeneracy and therefore, in higher tracking accuracy. For the radar tracking example with a realistic case, the proposed method has shown as much as 10.8% improvement in the RMSE,

9.7% reduction in the number of divergent tracks and 25% reduction in fail probability.

VI. DECLARATIONS

The authors declare no conflict of interest.

REFERENCES

- [1] N. Gordon, D. Salmond, and A. F. M. Smith, “Novel approach to nonlinear/non-Gaussian Bayesian state estimation,” *IEE Proc.-F*, vol. 140, no. 2, pp. 107–113, Apr. 1993.
- [2] M. S. Arulampalam, S. Maskell, N. Gordon, and T. Clapp, “A tutorial on particle filters for online nonlinear/non-Gaussian Bayesian tracking,” *IEEE Trans. Signal Process.*, vol. 50, no. 2, pp. 174–188, Feb. 2002.
- [3] B. Ristic, S. Arulampalam, and N. Gordon, *Beyond the Kalman Filter: Particle Filters for Tracking Applications*. Norwood, MA, USA: Artech House, 2003.
- [4] R. Douc and O. Cappe, “Comparison of resampling schemes for particle filtering,” in *Proc. 4th Int. Symp. Image Signal Process. Anal. (ISPA)*, 2005, pp. 64–69.

- [5] J. D. Hol, T. B. Schon, and F. Gustafsson, "On resampling algorithms for particle filters," in *Proc. IEEE Nonlinear Stat. Signal Process. Workshop*, Jul. 2006, pp. 79–82.
- [6] M. K. Pitt and N. Shephard, "Filtering via simulation: Auxiliary particle filters," *J. Amer. Stat. Assoc.*, vol. 94, no. 446, pp. 590–599, Jun. 1999.
- [7] A. M. Johansen and A. Doucet, "A note on auxiliary particle filters," *Statist. Probab. Lett.*, vol. 78, no. 12, pp. 1498–1504, 2008.
- [8] M. Pitt, R. S. Silva, P. Giordani, and R. Kohn, "On some properties of Markov chain Monte Carlo simulation methods based on the particle filter," *J. Econ.*, vol. 171, no. 2, pp. 134–151, 2012.
- [9] L.-Q. Li, W.-X. Xie, and Z.-X. Liu, "Auxiliary truncated particle filtering with least-square method for bearings-only maneuvering target tracking," *IEEE Trans. Aerosp. Electron. Syst.*, vol. 52, no. 5, pp. 2562–2567, Oct. 2016.
- [10] H. F. Lopes and R. S. Tsay, "Particle filters and Bayesian inference in financial econometrics," *J. Forecasting*, vol. 30, no. 1, pp. 168–209, 2011.
- [11] J. Liu, W. Wang, and F. Ma, "A regularized auxiliary particle filtering approach for system state estimation and battery life prediction," *J. Smart Mater. Struct.*, vol. 20, no. 7, 2011, Art. no. 075021.
- [12] J. P. Norton and G. V. Veres, "Improvement of the particle filter by better choice of the predicted sample set," *Proc. IFAC*, vol. 35, no. 1, pp. 365–370, 2002.
- [13] M. Lin, R. Chen, and J. S. Liu, "Lookahead strategies for sequential Monte Carlo," *J. Stat. Sci.*, vol. 28, no. 1, pp. 69–94, 2013.
- [14] A. C. Charalampidis and G. P. Papavassiliopoulos, "Improved auxiliary and unscented particle filter variants," in *Proc. 52nd IEEE Conf. Decis. Control*, Dec. 2013, pp. 7040–7046.
- [15] A. Melanie and P. J. Van Leeuwen, "An exploration of the equivalent weights particle filter," *Quart. J. Roy. Meteorological Soc.*, vol. 139, no. 672, pp. 820–840, 2013.
- [16] J. Kronander and T. B. Schön, "Robust auxiliary particle filters using multiple importance sampling," in *Proc. IEEE Workshop Stat. Signal Process. (SSP)*, Gold Coast, QLD, Australia, Jun. 2014, pp. 268–271.
- [17] V. Elvira, L. Martino, M. Bugallo, and P. M. Djuric, "Elucidating the auxiliary particle filter via multiple importance sampling," *IEEE Signal Process. Mag.*, vol. 36, no. 6, pp. 145–152, Jun. 2019.
- [18] N. Branchini and V. Elvira, "Optimized auxiliary particle filters: Adapting mixture proposals via convex optimization," in *Proc. Uncertainty Artif. Intell.*, 2021, pp. 1289–1299.
- [19] P. B. Choppala, "Auxiliary particle filtering with lookahead support for univariate state space models," *J. Annali Universita Ferrara*, vol. 70, pp. 515–532, Sep. 2024.
- [20] R. Gurajala, P. B. Choppala, J. S. Meka, and P. D. Teal, "A sorted weighting lookahead sampling scheme for accurate and fast particle filtering," in *Proc. 2nd Int. Conf. Range Technol. (ICORT)*, Chandipur, India, Aug. 2021, pp. 1–6.
- [21] O. D. Akyildiz and J. Míguez, "Nudging the particle filter," *J. Statist. Comput.*, vol. 30, pp. 305–330, Oct. 2020.
- [22] L. Xue, C. Na, and Y. Han, "Improved auxiliary particle filter for SINS/SAR navigation," *Math. Problems Eng.*, vol. 2021, pp. 1–9, Jan. 2021.



PRAVEEN B. CHOPPALA (Senior Member, IEEE) received the B.Tech., M.E., and Ph.D. degrees from Victoria University of Wellington, New Zealand, in 2005, 2008, and 2014, respectively. He held two postdoctoral positions, one at the University of Wellington, New Zealand, and the second with The University of New South Wales, Australia. Later, he moved to India. He is currently a Professor with the Department of Electronics and Communication Engineering, Andhra University. He is also a Visiting (Adjunct) Professor with Victoria University, Australia. His research interests include radar and sonar tracking, Bayesian filtering, and sequential Monte Carlo methods. He has authored over 60 publications and six books. He also holds one patent grant.



RAMONI ADEOGUN (Senior Member, IEEE) received the B.Eng. degree (Hons.) from the Federal University of Technology Minna, Nigeria, in 2007, and the Ph.D. degree from Victoria University of Wellington, Wellington, New Zealand, in 2015. From 2017 to 2021, he was a Postdoctoral Research Fellow with Aalborg University on multi-link radio channel modeling using propagation graphs. He is currently an Associate Professor with the Department of Electronic Systems, Aalborg University, Denmark. He is also in close collaboration with Nokia Bell Laboratories Aalborg as an External Research Engineer. He has authored over 80 publications and serves in various committees for reputed journals. His research interests include statistical signal processing and communication theory.